

Chapter 2

Pairing with transfer

2.1 Nuclear Structure in a nutshell

handwritten
pp. 103a - 103c
Kofb. 7/4/16
14/4/16

The low-energy properties of quantal, many-body, Fermi systems displaying sizable values of zero-point-motion (kinetic energy) of localization compared to the strength of the NN -interaction and quantified by the quantality parameter $q \gtrsim 0.15$ (see App. 2.3, and 2.6 Fig. 2.3.1, Fig. 2.6.2 and Fig. 2.6.3 Table 2.3.1), are determined by the laws which control independent-particle fermion motion close to the Fermi energy ϵ_F , and by the relations/correlations operating among these fermions. First of all, the Pauli principle, implying orbitals solidly anchored to the single-particle mean field, as testified by the Hartree-Fock ground state $|HF\rangle = \prod_i a_i^\dagger |0\rangle$ (Figs. 2.3.2 and 2.3.3), describing a step function separation in the probability of occupied ($\epsilon_i \leq \epsilon_F$) and empty ($\epsilon_k \geq \epsilon_F$) states.

Pairing acting on fermions moving in time reversal states lying close to ϵ_F alters this picture in a conspicuous way (cf. e.g. Broglia, R. A. and Zelevinsky, V. (2013)). In particular, in the case of $S = 0$ configurations, in which case the radial component of the pair wavefunction does not display nodes. Within an energy range of the order of the pair correlation energy $E_{corr} (\approx -(N(0)/2)\Delta^2$ within BCS) centered around $\epsilon_F (E_{corr}/\epsilon_F \ll 1)$ the system is now made out of pairs of fermions which flicker in and out of the correlated ($L = 0, S = 0$) configuration (Cooper pairs (Cooper (1956)), App. 2.6 cf. also Brink, D. and Broglia (2005), in particular Apps. A.G.H.I and J of this reference). For temperatures (intrinsic excitation energies) or stress regimes (magnetic field in metals, Coriolis force in nuclei, etc.) smaller than $\approx |E_{corr}/2|$ (\approx critical value), Cooper pairs respect Bose-Einstein statistics (BCS condensation of Figs. 2.3.4 and 2.3.5), the single-particle orbits on which they are correlated become dynamically detached from the mean field, leading to a bosonic-like condensate and, at the same time, reducing in a conspicuous way the inertia of the system. For example the moment of inertia I of quadrupole rotational bands of superfluid nuclei with open shells of both protons and neutrons is found to be considerably smaller than the rigid moment of inertia I_r ($I \approx I_r/3$) expected from independent-particle motion (Inglis limit; see Figs. 2.3.4 and 2.3.5). The observed values however, are about a factor of 2 larger than the rotational moment of inertia. (Belyaev (1959), Belyaev, S. T. (2013), Bohr and Motteux (1975))

- ① Broglia Zelevinsky
- ② Cooper
- ③ Brink and Broglia
- ④ Belyaev (1959), Belyaev, S. T. (2013), Bohr and Motteux (1975)

The low-energy properties of the finite, quantal, many-body nuclear system, in which nucleons interact through the strong force of strength $v_0 (\approx -100 \text{ MeV})$ and range $a (\approx 1 \text{ fm})$ are controlled, in first approximation by independent particle motion. This is a consequence of the fact that nucleons display a sizable value of the zero point (kinetic) energy of localization ($\hbar^2/Ma^2 \approx 40 \text{ MeV}$) as compared to the absolute value of the strength of the NN-potential^{*} $|V_0| = 100 \text{ MeV}$.

The corresponding ground state $|\text{HF}\rangle = \prod_i |\alpha_i; 10\rangle$ describes a step function in the probability of the occupied ($E_i \leq E_F$) and empty ($E_k > E_F$) states. Pushing the system it reacts with an inertia AM , sum of the nucleon masses. Setting it into rotation, assuming the density $P(r) = \sum_i |\langle \vec{r} | i \rangle|^2$ ($|i\rangle = \alpha_i; 10\rangle$) to be spatially deformed, it responds with the rigid moment of inertia. This is because the single-particle orbitals are solidly anchored to the mean field.

The generalization to aperiodic crystals, like e.g., proteins (Schrödinger (1944)) was carried out in Stillinger and Stillinger (1990). Its application to the atomic nucleus is discussed in detail.

*) The corresponding ratio $q = (\frac{\hbar^2}{Ma^2}) \frac{1}{|V_0|}$ is known in connection with the study of condensed matter (de Boer (1948), (1957), de Boer and Lundbeck (1948), Nasanov (1976)). It was introduced in nuclear physics in Mottelson (1998) where its value $q=0.4$ testifies to the validity of independent particle motion. It is of notice that questions like the one posed in connection with localization and long mean free path were already discussed by Lindemann (1910) in connection with the study of the stability or less of crystals.

Pairing acting on nucleons moving in time reversal states $\nu, \bar{\nu}$ ($\nu \equiv (nlj)$), in configurations of the type $(l)_{L=0}^2, (s)_{S=0}^2$, and lying close to the Fermi energy

- ① $E_F (\approx 36 \text{ MeV})$, alter this picture in a conspicuous way.¹ Within an energy range of the order of the absolute value of the pair correlation energy² $E_{\text{corr}} (\approx -3 \text{ MeV})$ centered around E_F ($|E_{\text{corr}}|/E_F \ll 1$), the role of independent particles is taken over by independent pairs of nucleons, correlated over distances $\xi \approx \hbar v_F / (2\Delta) (\approx 30 \text{ fm})$, which flicker in and out of the corresponding $L=0, S=0$ configuration (Cooper pairs^{3,4}).

- ② For intrinsic⁵ nuclear excitation energies and rotational frequencies⁶ smaller than $|E_{\text{corr}}|/2$ and $\hbar\omega_{\text{rot}} \approx 0.5 \text{ MeV}$ respectively, the system can be described in terms of independent pair motion. This is a

¹R.A.Broglia and V.Zelevinsky (2013)

² In BCS, $E_{\text{corr}} \approx N(0) \Delta^2$, where $N(0) = \frac{g}{2}$ is the density of states at the Fermi energy and for one spin orientation, $g_i = i/16 \text{ MeV}^{-1}$ ($i=N, Z$) being ^{the result of} an empirical estimate which takes surface effects into account (Bohr and Mottelson (1975), Bortignon et al (1998)), while Δ is the pairing gap. For a typical superfluid, quadrupole deformed nucleus like ¹⁷⁰Yb, $N(0) = 5.3 \text{ MeV}^{-1}$, $\Delta \approx 1.1 \text{ MeV}$ and $E_{\text{corr}} = -3.2 \text{ MeV}$ (Shimizu et al (1989)).

³ Cooper (1957)

⁴ Brunk and Broglia (2005) excitations

⁵ As opposed to collective excitations, which do not alter the temperature of the system.

⁶ Coriolis force acts oppositely on each member of a Cooper pair. When the difference in rotational energy between superfluid and normal rotation becomes about equal to the correla-

Kob 14/04/16

consequence of the fact that the kinetic energy (103) of (Cooper) pair confinement ($\frac{\hbar^2}{2M\zeta^2} \approx 10^{-2}$ MeV) is much smaller than the absolute value of the pair binding energy $|E_{\text{corr}}|$, implying that each pair behaves as an entity⁷ of mass $2M$ and spin $S=0$. Cooper pairs respect Bose-Einstein statistics, the single-particle orbits on which they correlate become dynamically detached from the mean field, leading to a bosonic-like condensate. This has a number of consequences. In particular, the moment of inertia I of quadrupole rotational bands of superfluid nuclei with open shells of both protons and neutrons is found to be smaller than the rigid moment of inertia by a factor of 2. The observed values, however, are a factor of 5 larger^{than} the irrotational moment of inertia⁸, testifying to a subtle interplay between pairing and shell effects.

tion energy, the nucleon moving opposite to the collective rotation becomes so much retarded in its revolution around with respect to the partner nucleon, that eventually it cannot correlate any more with it and "align" its motion (and spin) with the rotational motion, becoming again a pair of fermions and not participating any more in the condensate. This happens for a (critical) angular momentum $I_c \approx (120 \times |E_{\text{corr}}|)^{1/2} \approx 20\hbar$, corresponding to a rotational frequency $\hbar\omega_c \approx 0.5$ MeV (Brink and Broglie (2005)).

8 Bohr A. and Mottelson (1975), Belyaev (1959), Belyaev S.T (2013)

7. The ratio $q_\zeta = \frac{\hbar^2}{2M\zeta^2} \frac{1}{|E_{\text{corr}}|} \approx 0.007$ provides a generalized quantity parameter. It testifies to the stability of nuclear Cooper pairs in superfluid nuclei. (a)

(c) provides one of the clearest quantitative examples of the central and ubiquitous role pairing vibrations play in nuclear pairing correlations. (c) top.
138

2.1. NUCLEAR STRUCTURE IN A NUTSHELL

105

2.3.3 and 2.6.2; cf. Belyaev (1959), Belyaev, S. T. (2013) Bohr, A. and Mottelson (1975) and references therein; within this context see last paragraph of App. 2.6).

Cooper pairs exist also in situations in which the environmental conditions are above critical, e.g. in metals at room temperature, in closed shell nuclei as well as in deformed open shell ones at high values of the angular momentum, although they break as soon as they are generated (pairing vibrations). While these pair addition and subtraction fluctuations have little effect in condensed matter systems with the exception than at $T \approx T_c$ (Schmid, A. (1966), Schmidt, H. (1968), Schmid, A. (1969) Abrahams, E. and Woo (1968); concerning superfluid ^3He cf. Wölfe, P. (1978)), they play an important role in mesoscopic systems. In particular in nuclei around closed shells (Fig. 2.1.1) and App. 2.7, Fig. 2.7.8 specially in the case of light, highly polarizable, exotic halo nuclei (see App. 2.8; Bohr, A. and Mottelson (1975), Bès, D. R. and Broglia (1966), Högaasen-Feldman (1961), Schmidt, H. (1972), Schmidt, H. (1968), Barranco, F. et al. (2001), Potel, G. et al. (2013a), Potel et al. (2014)). From this vantage point of view one can posit that it is not so much, or, at least not only, the superfluid state which is abnormal in the nuclear case, but the normal state associated with closed shell systems.¹⁰⁾ It is of notice nonetheless, the role pairing vibrations play in the transition between superfluid and normal nuclear phases (cf. Fig. 2.1.2) as a function of the rotational frequency (angular momentum) as emerged from the experimental studies of high spin states carried out by, among others, Garrett and collaborators¹¹⁾ (cf. Shimizu, Y. R. et al. (1989); cf. also Brink, D. and Broglia (2005), Ch. 6 and references therein).

From Fig. 2.1.2 it is seen that while the dynamic pairing gap associated with pairing vibrations leads to a $\approx 20\%$ increase of the static pairing gap for low rotational frequencies, it becomes the overwhelming contribution above the critical frequency (Shimizu, Y. R. et al. (1989), Shimizu, Y. R. and Broglia (1990), Shimizu, Y. R. (2013), Dönau, F. et al. (1999) Shimizu, Y. R. et al. (2000)). In any case, the central role played by pairing vibrations within the present circumstances is that to restore particle-number conservation, an example of the fact that potential functionals are, as a rule, best profited by special arrangements of fermions (spontaneous symmetry breaking), while fluctuations restore symmetry (cf. Chapter 6 Section 6.2.3). Within this context, there are a number of methods which allows one to go beyond mean-field approximation (HFB). Generally referred to as number projection methods (NP), they make use of a variety of techniques (Generator Coordinate Method, Pfaffians, etc.) as well as protocols (variation after projection, gradient method, etc.).¹²⁾ Ring, P. and Schuck (1980), Egido, J. L. (2013), Robledo, R. M. and Bertsch (2013); cf. also Frauendorf, S. (2013), Ring, P. (2013), Heenen, P. H. et al. (2013), and references therein). The advantages of NP methods over the RPA is to lead to smooth functions for both the correlation energy and the pairing gap at the pairing phase transition between normal and superfluid phases. That is, between the pairing vibrational and pairing rotational schemes (Figs. 2.1.1, 2.1.3, 2.1.4, see also Fig. 2.6.1)¹³⁾ Bès, D. R. and Broglia (1966), Bohr, A. and Mottelson (1975) and references therein).

The above results underscore the fact that, at the basis of an operative coarse

→ 12)

→ 13) Anderson (1984); see Ch. 6, Sect. 6.2.3
(P.W. Anderson, Basic Notions of Condensed Matter,
Addison Wesley, Reading MA (1997),

10) see Potel et al. (2013) and refs. therein. Also

Potel et al. [87, 0544321 (2013)] in connection with
the closed shell system ^{132}Sn .

11)

(undone)

nuclei

and

Sects. 2.7
and

— italics

another

after that provided
by the quantity
parameter and
its generalization
to pair motion,

→ 15

footnote
14

and Sects.
2.6.2 and 2.7

footnote 15

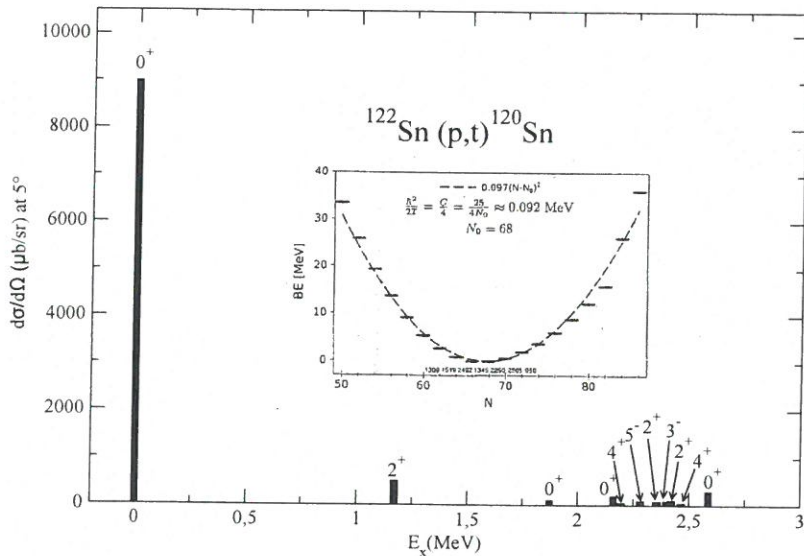


Figure 2.1.3: Excitation function associated with the reaction $^{122}\text{Sn}(p, t)^{120}\text{Sn}(J^\pi)$. The absolute experimental values of $d\sigma(J^\pi)/d\Omega|_{5^\circ}$ are given as a function of the excitation energy E_x (after Guazzoni, P. et al. (2011)). In the inset the full neutron pairing rotational band between magic numbers $N = 50$ and $N = 82$ is also displayed, the absolute $^{A+2}\text{Sn}(p, t)^A\text{Sn}$ experimental cross sections are reported in the abscissa (Guazzoni, P. et al. (1999), Guazzoni, P. et al. (2004), Guazzoni, P. et al. (2006), Guazzoni, P. et al. (2008), Guazzoni, P. et al. (2011), Guazzoni, P. et al. (2012); see also Potel, G. et al. (2011), Potel, G. et al. (2013b)).

(within this context cf. App. D, in particular the discussion following Eq (1.0.5))

grained approximation to the nuclear many-body problem one finds a judicious choice of the collective coordinate/s¹. In other words, pairing vibrations are elementary modes of excitation containing the right physics to restore gauge invariance through their interweaving with quasiparticle states. Within the framework of the above picture, one can introduce at profit a collective coordinate α_0 (order parameter) which measures the number of Cooper pairs participating in the pairing condensate, and define a wavefunction for each pair $(U_\nu + V_\nu d_\nu^\dagger d_{\bar{\nu}}^\dagger)|0\rangle$ (independent pair motion, BCS approximation, cf. Figs. 2.6.1, 2.6.2 and 2.6.3), adjusting the occupation parameters V_ν and U_ν (probability amplitudes that the two-fold, Kramer's-degenerate pair state $(\nu, \bar{\nu})$, is either occupied or empty), so as to minimize the energy of the system under the condition that the average number of nucle-

¹ Within this context we quote allegedly from E. Wigner: "In solving a problem you may choose to use the degrees of freedom you like. But if you choose the wrong ones you will be sorry".

In this connection,

? gregory weinberg ?

ons is equal to N_0 (the Coriolis-like force felt, in the intrinsic system in gauge space by the Cooper pairs, being equal to $-\lambda N_0$). Thus, $|BCS\rangle = \prod_{\nu>0} (U'_\nu + V'_\nu a_\nu^\dagger a_\nu^\dagger) |0\rangle$ provides a valid description of the independent pair mean field ground state, and of the associated order parameter $\alpha_0 = \langle BCS | P^\dagger | BCS \rangle = \sum_{\nu>0} U'_\nu V'_\nu$, $P^\dagger = \sum_{\nu>0} a_\nu^\dagger a_\nu^\dagger$ being the pair creation operator (cf. Bardeen et al. (1957a), Bardeen et al. (1957b), Schrieffer (1964), Schrieffer, J. R. (1973) and references therein). It is then natural to posit that two-particle transfer reactions are specific to probe pairing correlations in many-body fermionic systems. Examples are provided by the Josephson effect (Josephson (1962)) between e.g. metallic superconductors, and (t, p) and (p, t) reactions in atomic nuclei (cf. e.g. Yoshida (1962), Broglia, R.A. et al. (1973), Bayman (1971), Glendenning, N. K. (1965), Bohr (1964), Hansen (2013) and Potel, G. et al. (2013a) and references therein; cf. also Figs. 2.1.3 and 2.1.4.)

(A) - (A) from pp. 109a - 109b Kbhvn 15/4/16

Due to the fact that, away from the Fermi energy pair motion becomes independent particle motion (see App. 2.6), one-particle transfer reactions like e.g. (d, p) and (p, d) can be used together with (t, p) and (p, t) processes as valid tools to cross check pair correlation predictions (see Chapter 4). In particular, to shed light on the origin of pairing in nuclei: in a nutshell, the relative importance of the bare NN -interaction and the induced pairing interaction (within this context see App. 2.8).

Sect.

While the calculation of two-nucleon transfer spectroscopic amplitudes and differential cross sections are, a priori, more involved to be worked out than those associated with one-nucleon transfer reactions, the former are, as a rule, more "intrinsically" accurate than the latter ones. This is because, in the case of two nucleon transfer reactions, the quantity (order parameter α_0) which expresses the collectivity of the members of a pairing rotational band reflect the properties of a coherent state ($|BCS\rangle$). In other words, it results from the sum over many contributions ($\sqrt{j_\nu + 1/2} U'_\nu V'_\nu$, cf. App. 2.6), all of them having the same phase. Consequently, errors are averaged out in the summed value $|\alpha_0|$, conferring the two-nucleon transfer cross section $d\sigma(2n \text{ transfer})/d\Omega \sim |\alpha_0|^2$, a quantitative accuracy which goes beyond that of the individual contributions. On the other hand, $d\sigma(1n\text{-transfer})/d\Omega \sim |U'_\nu|^4 (\sim |V'_\nu|^4)$ depends on the accuracy with which one is able to calculate the occupancy of a single pure configuration (similar to the relative accuracy with which one can calculate the nuclear density as a whole and the density associated with a single orbital, quantities which can be probed in (e, e') experiments).

Sect.

(Z) - (Z) pp. 109c 109e Kbhvn 19/4/16

The soundness of the above parlance reflects itself in the calculation of the elements resulting from the encounter of structure and reaction, namely one- and two-nucleon modified transfer formfactors. While it is usually considered that these quantities carry all the structure information associated with the calculation of the corresponding cross sections, a consistent NFT treatment of structure and reaction will posit that equally much is contained in the distorted waves describing the relative motion of the colliding systems. This is because the optical potential ($U + iW$) which determines the scattering waves, emerges from the same

2

3

4

(A)

Within this context we now take up the basic consequence of pairing condensation in nuclei regarding reaction mechanisms. (from p. 109^b)

Let us assume that projectile and target are in such a weak contact throughout the entire reaction process, so as to only allow for single-nucleon transfer with any appreciable cross section. (from p. 109^c)

in superfluid nuclei

Because $(\hbar^2/2M\epsilon^2)/|E_{\text{corr}}| \approx 10^{-2}$, Cooper pairs behave as particles of mass $2M$ over distances ξ , even in the case in which the NN-potential vanishes in the zone between the weakly overlapping densities of the two interacting nuclei. (from p. 109^d)

As a consequence one expects Cooper pair transfer to be observable, observed through

observability

and successive transfer to

probe pair correlations equally well than simultaneous transfer.

Because $\sigma_0 \sim N(0)$, cross sections associated with the transfer of Cooper pairs between members of a pairing rotational band, are proportional to the density of single-particle levels quantity squared. As a consequence, absolute two-nucleon transfer cross sections are expected to be of the same order of magnitude than one-nucleon transfer ones, and to be dominated by successive transfer. These expectations have been confirmed experimentally and by detailed numerically calculations respectively.

The above parlance, being at the basis of the Josephson effect, reflects both one of the most solidly established results in the study of BCS pairing, and explains the workings of a paradigmatic probe of spontaneous symmetry breaking phenomena.

(A) to p. 109

(α) For this purpose let us consider a gedanken experiment in which the superfluid target and the projectile can at best come in such weak contact that only single-nucleon transfer leads to a yield falling within the sensitivity range of the measuring setup. (α) to p. 109a

(β) One then expects Cooper pair transfer to be observed. Not only. One also expects that the associated absolute differential cross section contains, for the particular choice of mass number done and within the framework of the theory of quantum measurement, all the information needed to work out a comprehensive description of nuclear superfluidity. (β) to p. 109a

② consequently, the relative error decreases as the square root of the number of contributions ($\approx N(0) \Delta \approx 4 \text{ MeV}^{-1} \times 1.4 \text{ MeV} \approx 6$ in the case of the superfluid nucleus ^{120}Sn).

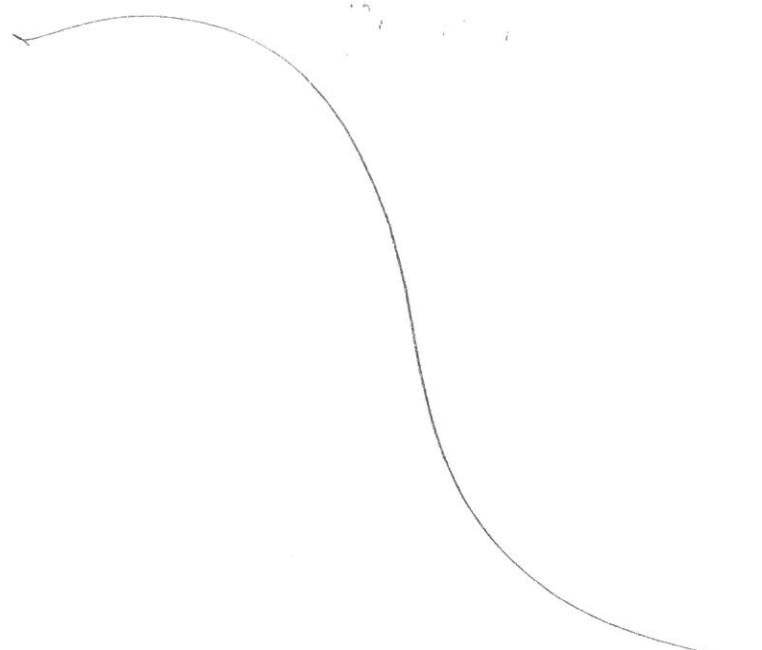
There is a further reason which confers $d_0' = \sum_j (j+1/2) U'_j V'_j$ a privileged position with respect to the single contributions $(j+1/2) U'_j V'_j$. It is the fact that $d_0' = e^{2i\phi} \sum_j (j+1/2) U_j V_j = e^{2i\phi} d_0$ defines a privileged orientation in gauge space, d_0 being the order parameter referred to the laboratory system which makes an angle ϕ in gauge space with respect to the intrinsic system to which d_0' is referred.*). In other words, the quantities d_0' (the deformation of the superfluid nuclear system in gauge space, and the rotational frequency $\lambda = \hbar\phi$ in this space and associated Coriolis force $-\lambda N_0$ felt by the nucleons referred to the body fixed frame) are the result of solving selfconsistently the BCS number and gap equations $N_0 = \sum_j (2j+1) \left(1 - \frac{(E_j - \lambda)/\Delta}{\sqrt{1 + ((E_j - \lambda)/\Delta)^2}}\right)$ and $d_0' = \sum_j (j+1/2) U'_j V'_j = \sum_j (j+1/2) \left(1 - \frac{1}{\sqrt{1 + ((E_j - \lambda)/\Delta)^2}}\right)$ making use as inputs E_j , N_0 and Δ , that is single-particle energies, average number of particles and pairing gap.

Similar arguments can be used.

*) See Sect. 2.6.2, see Potel et al (2013b)

KBRM 19/04/16

regarding the excitation of pairing vibrations in terms of Cooper pair transfer from closed shells as compared to one-particle transfer. As seen from Fig. 2.1.5 (b)-(c), the random phase approximation (RPA) amplitudes X_v^a and Y_v^a sum coherently over pairs of time reversal states, to give rise to the direct excitation of the pair addition mode displayed in (d). Because of the (dispersion) relation $(b)+(c) \equiv (d)$, X_v - and Y_v - amplitudes are correlated among themselves as well as between them, both in amplitude as well as in phase. As seen from (g) and (h), the situation is quite different in the case of one-particle transfer.



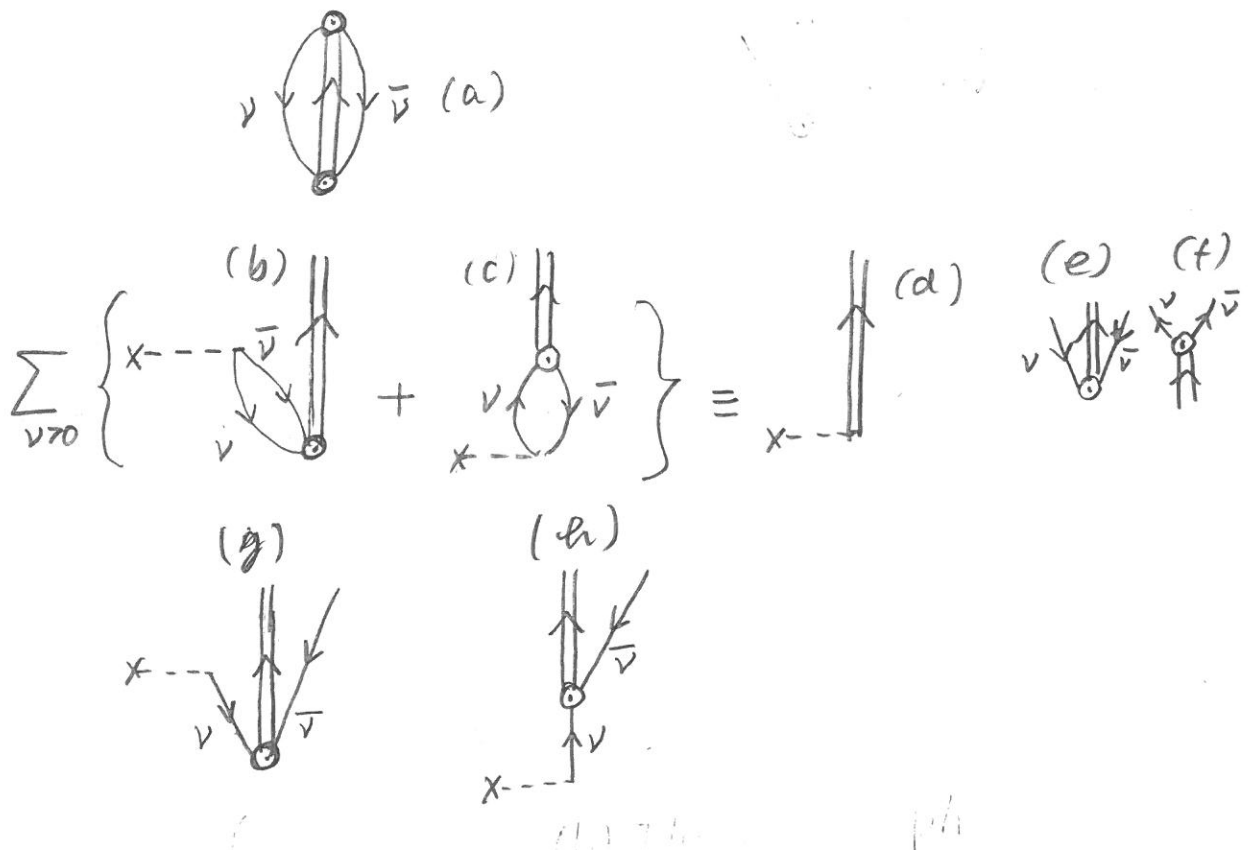


Fig. 2.1.5 NFT diagrams associated with one- and two-particle transfer from closed shell. (a) ZPF associated with the virtual excitation of a pair addition mode and two uncorrelated holes. (c) two-particle transfer filling the holes, (c) obtain from the previous graph by time ordering. These processes receive contribution from all $(\nu, \bar{\nu})$ pairs (sum over $\nu \bar{\nu}$), leading to (d) the direct excitation of the pair addition mode. The relation $(b) + (c) \equiv (d)$ is the NFT graphical representation of the random phase approximation (RPA) dispersion relation to calculate the properties of the pair addition mode in the harmonic approximation (Section 2.7). The backward and forward-going amplitudes are displayed in Figs. (e) and (f) respectively. (g) One-particle stripping proceeding through the transfer to a hole associated with the ZPF. (h) processes obtained from the previous one by time ordering.

(2)

modified formfactors, eventually including also inelastic processes (cf. App. 3.5; cf also Broglia, R. A. et al. (1981), Pollaro et al. (1983), Broglia and Winther (2004), Fernández-García, J.P. et al. (2010), Fernández-García, J.P., M. Rodríguez-Gallardo et al. (2010), Dickhoff, W. and Van Neck (2005), Jenning, B. (2011), Montanari et al. (2014)). In other words, to describe a two-nucleon transfer reaction like $A + t \rightarrow B (= A + 2) + p$, one needs to know what the single-particle states and collective modes of the system $F (= A + 1)$ are, equally well than those of nuclei A and B . In principle, also the deuteron wavefunction as one knows the triton wavefunction (see Chapter 3, cf. also Chapter 5, Section 5.1). Furthermore one needs to take into account the interweaving of different modes and degrees of freedom resulting in dressed particle states (quasiparticles; fermions) and renormalized normal vibrational modes of excitation (bosons). But these are essentially all the elements needed to calculate the processes leading to the depopulation of e.g. the flux in the incoming channel ($A + t$ in the case under discussion). In particular, and assuming to work with spherical nuclei, one-particle transfer is, as a rule, the main depopulation process. This is a consequence of the long range tail of the associated formfactors as compared to that of other processes, e.g. inelastic processes (cf. e.g. Fig. 3.5.5).

In keeping with this fact, and because U and W are connected by the Kramers-Krönig generalized dispersion relation (fluctuation-dissipation theorem, see e.g. Mahaux, C. et al. (1985) and references therein), it is possible to calculate the nuclear dielectric function (optical potential) associated with the elastic channels under discussion (i.e. (A, t) , (F, d) and (B, p) in the present case) making use of the above described elements.

Concerning the modified formfactor associated with e.g. a (t, p) process, we shall see in the (Chapter 5, App. 5.3) that it can be written as

$$u_{LSJ}^{J_i J_f}(R) = \sum_{\substack{n_1 l_1 j_1 \\ n_2 l_2 j_2, n}} B(n_1 l_1 j_1, n_2 l_2 j_2; J J_i J_f) \\ \times \langle S L J | j_1 j_2 J \rangle \times \langle n 0, N L, L | n_1 l_1, n_2 l_2; L \rangle \\ \times \Omega_n R_{NL}(R), \quad (2.1.1)$$

where the overlaps

$$B(n_1 l_1 j_1, n_2 l_2 j_2; J J_i J_f) \\ = \langle \Psi^{J_f}(\xi_{A+2}) | [\phi^J(n_1 l_1 j_1, n_2 l_2 j_2), \Psi^{J_i}(\xi_A)]^{J_f} \rangle, \quad (2.1.2)$$

and

$$\Omega_n = \langle \phi_{nlm_l}(\mathbf{r}) | \phi_{000}(\mathbf{r}) \rangle, \quad (2.1.3)$$

encode for the physics of particle-particle (but also, to a large extent, particle-hole) correlations in nuclei, $\langle S L J | j_1 j_2 J \rangle$ and $\langle n 0, N L, L | n_1 l_1, n_2 l_2; L \rangle$ being $LS - jj$ and Moshinsky transformation brackets, keeping track of symmetry and number of degrees of freedom conservation (Glendenning, N. K. (1965), Broglia, R.A. et al.

5

6

7

(1973)) In fact, the two-nucleon spectroscopic amplitude (B-coefficient) and the overlap Ω_n reflect the parentage with which the nucleus B can be written in terms of the system A and a Cooper pair,

$$\Psi_{exit} = \Psi_{M_f}^{J_f}(\xi_{A+2}) \times \chi_{M_{S_f}}^{S_f}(\sigma_p), \quad (2.1.4)$$

where

$$\begin{aligned} \Psi_{M_f}^{J_f}(\xi_{A+2}) &= \sum_{\substack{n_1 l_1 j_1 \\ n_2 l_2 j_2 \\ J, J'_i}} B(n_1 l_1 j_1, n_2 l_2 j_2; J J'_i J_f) \\ &\times [\phi^J(n_1 l_1 j_1, n_2 l_2 j_2) \Psi_i^{J'_i}(\xi_A)]_{M_f}^{J_f}, \end{aligned} \quad (2.1.5)$$

and

$$\Psi_{entrance} = \Psi_{M_i}^{J_i}(\xi_A) \times \phi_i(\mathbf{r}_{n1}, \mathbf{r}_{n2}, r_p; \sigma_{n1}, \sigma_{n2}, \sigma_p), \quad (2.1.6)$$

with

$$\phi_i = [\chi^S(\sigma_{n1}, \sigma_{n2}) \chi^{S'_i}(\sigma_p)]_{M_{S_i}}^{S_i} \times \phi_i^{L=0} \left(\sum_{i>j} |\mathbf{r}_i - \mathbf{r}_j| \right). \quad (2.1.7)$$

Assuming for simplicity a symmetric di-neutron radial wavefunction for the triton (i.e. neglecting the d -component of the corresponding wavefunction) both for the relative and for the center of mass wavefunctions $\phi_{nlm}(\mathbf{r})$ and $\phi_{N\Lambda M}(R)$ ($n = l = m = 0, N = \Lambda = M = 0$), leads to Ω_n , a quantity which reflects both the non-orthogonality existing between the di-neutron wavefunctions in the final nucleus (Cooper pair) and in the triton as well as their degree of s -wave of relative motion. Another way to say the same thing is to state that dineutron correlations in these two systems are different, a fact which underscores the limitations of light ion reactions to probe specifically pairing correlations in nuclei (within this context see von Oertzen and Vitturi (2001), von Oertzen, W. (2013)).

One can then conclude that, provided one makes use of a (sensible) complete single-particle basis (eventually including also the continuum), one can capture through $u_{LSJ}^{J_i J_f}(R)$ most of the coherence of Cooper pair transfer, as a major fraction of the associated di-neutron non-locality is taken care of by the n -summation appearing in eq. (2.1.1), the different contributions being weighted by the non-orthogonality overlaps Ω_n . This is in keeping with the fact that, making use of a more refined triton wavefunction than that employed above, the $n - p$ (deuteron-like) correlations of this particle can be described with reasonable accuracy and thus, the emergence of successive transfer (see Chapter 3). On the other hand, being the deuteron a bound system, this effective treatment of the associated resonances is not particularly economic. Furthermore, it is of notice that the zero-range approximation ($V(\rho)\phi_{000}(\rho) = D_0\delta(\rho)$) eliminates the above mentioned possibilities cf. eq. (5.3.19).

Anyhow, the fact that one can still work out a detailed and physically insightful picture of two-nucleon transfer reactions in nuclei in terms of absolute cross sections with the help of a single parameter ($D_0^2 \approx (31.6 \pm 9.3)10^4 \text{ MeV}^2 \text{ fm}^2$) testifies to

the fact that the above picture of Cooper pair transfer (Glendenning, N. K. (1965), Bayman and Kallio (1967)) is a useful one, as it contains a large fraction of the physics which is at the basis of Cooper pair transfer in nuclei (Broglia, R.A. et al. (1973)). This is in keeping with the fact that the Cooper pair correlation length is much larger than nuclear dimensions and, consequently, simultaneous and successive transfer feel the same pairing correlations (see Chapter 3). In other words, treating explicitly the intermediate deuteron channel in terms of successive transfer, correcting both this and the simultaneous transfer channels for non-orthogonality contributions, makes the above picture the quantitative probe of Cooper pair correlations in nuclei (Fig. 2.21, Bayman and Chen (1982) and Potel, G. et al. (2013a)).

Within the above context, we provide below two examples of B -coefficients associated with coherent states. Namely, one for the case in which A and $B (= A+2)$ are members of a pairing rotational band. A second one, in the case in which they are members of a pairing vibrational band. That is,

$$1), B(nlj, nlj; 000) = \langle BCS(N+2) | [a_{nlj}^\dagger a_{nlj}^\dagger]_0^0 | BCS(N) \rangle = \sqrt{j+1/2} U_{nlj}(N) V_{nlj}(N+2), \quad (2.1.8)$$

and

$$2), B(nlj, nlj; 000) = \langle (N_0 + 2)(gs) | [a_{nlj}^\dagger a_{nlj}^\dagger]_0^0 | N_0(gs) \rangle$$

$$\text{Sect} \quad = \begin{cases} \sqrt{j_k + 1/2} X^a(n_k l_k j_k) & (\epsilon_{j_k} > \epsilon_F) \\ \sqrt{j_k + 1/2} Y^a(n_i l_i j_i) & (\epsilon_{j_k} \leq \epsilon_F) \end{cases} \quad (2.1.9)$$

Where the X and Y coefficients are the forwardgoing and backwardsgoing RPA amplitudes of the pair addition mode. For actual numerical values see App. 2.6, Table 2.6.1 and App. 2.7 Tables 2.7.2–2.7.5.

We conclude this section by remarking that, in spite of the fact that one is dealing with the connection between structure and direct transfer reactions, no mention has been made of spectroscopic factors in relation with one-particle transfer processes, let alone when discussing two-particle transfer. In fact, one will be using throughout the present monograph, exception made when explicitly mentioned, absolute cross sections as the sole link between spectroscopic amplitudes and experimental observations.

Renormalization and spectroscopic amplitudes. 2.2 Connection between theory and experiment

Let us elaborate on the above question in connection with one-particle transfer reactions (Mahaux, C. et al. (1985), Brink, D. and Broglia (2005) and references therein; cf. also App. 4.F). Elementary modes of nuclear excitation, namely single-particle motion, vibrations and rotations, being tailored to economically

Let us

9

10

11

describe the nuclear response to external probes, contain a large fraction of the many-body correlations. Consequently, their wavefunctions are non-orthogonal to each other, in keeping with the fact that all the degrees of freedom of the nucleus are exhausted by those of the nucleons (see Chapter 1). The resulting overlaps give a measure of the strength with which the different modes couple to each other. The resulting particle-vibration coupling Hamiltonian can be diagonalized, making use of Nuclear Field Theory (NFT, cf. Bortignon, P. F. et al. (1977), Bortignon, P. F. et al. (1978)), and of the BRST techniques in the case of particle-rotor coupling (cf. Bes, D. R. and Kurchan (1990)) or, approximately in terms of large amplitude plastic-like vibrations (cf. end of Sect. 2.6.1 and App. 2.4).

As a result of the interweaving of single-particle and collective motion, the nucleons acquire a state dependent self energy $\Delta E_j(\omega)$ which, for levels far away from the Fermi energy can become complex. Consequently, the single-particle potential which was already non-local in space (exchange potential, related to the Pauli principle) becomes also non-local in time (retardation effects; cf. e.g. Fig 2.8.3 (I) also Fig. 4.B.1). There are a number of techniques to make it local. In particular the Local Density Approximation (LDA) and the effective mass approximation. In this last case one can describe the single-particle motion in terms of a local (complex) potential with a real part given by $U'(r) = (m/m^*)U(r)$, where $m^* = m_k m_\omega / m$ is the effective nucleon mass, m_k being the so-called k -mass (non-locality in space in keeping with the fact that $\Delta x \Delta k_x \geq 1$), and $m_\omega = m(1 + \lambda)$ being the ω -mass (non-locality in time, as implied by the relation $\Delta \omega \Delta t \geq 1$), $\lambda = -\partial \Delta E(\omega) / \partial \hbar \omega$ being the so-called mass enhancement factor. It reflects the ability with which vibrations cloth single-particles. In other words, it measures the probability with which a nucleon moving at $t = -\infty$ in a "pure" orbital j can be found at a later time in a $2p - 1h$ like (doorway state) $|j'L; j\rangle$, L being the multipolarity of a vibrational state. Within this context, the discontinuity taking place at the Fermi energy in the dressed particle picture ($Z_\omega = (m/m_\omega)$; cf. Appendix D introducción) is connected with the single-particle occupancy probability.

It is of notice that dressed particles (cf. e.g. Fig. 2.8.3 (I) also Fig. 4.B.1) automatically imply an induced pairing interaction (cf. e.g. Fig. 2.8.3 (II) and Fig. 4.2.6 (b)) resulting from the exchange of the clothing vibrations between pairs of nucleons moving in time reversal states close to the Fermi energy. In other words, fluctuations in the normal density ($\delta \rho$, cf. Fig. 4.A.1 (i)) and the associated particle-vibration coupling vertices lead to abnormal (superfluid) density (deformation in gauge space). Whether this is a dynamic or static effect, depends on whether the parameter (cf. Fig. 2.7.7)

$$x' = G' N'(0), \quad (2.2.1)$$

product of the effective pairing strength,

$$G' = Z_\omega^2 (v_p^{bare} + v_p^{ind}), \quad (2.2.2)$$

and of the renormalized density of levels $N'(0)$ is considerable smaller (larger) than $\approx 1/2$. The quantity G' is the sum of the bare and induced pairing interaction,

→ 12

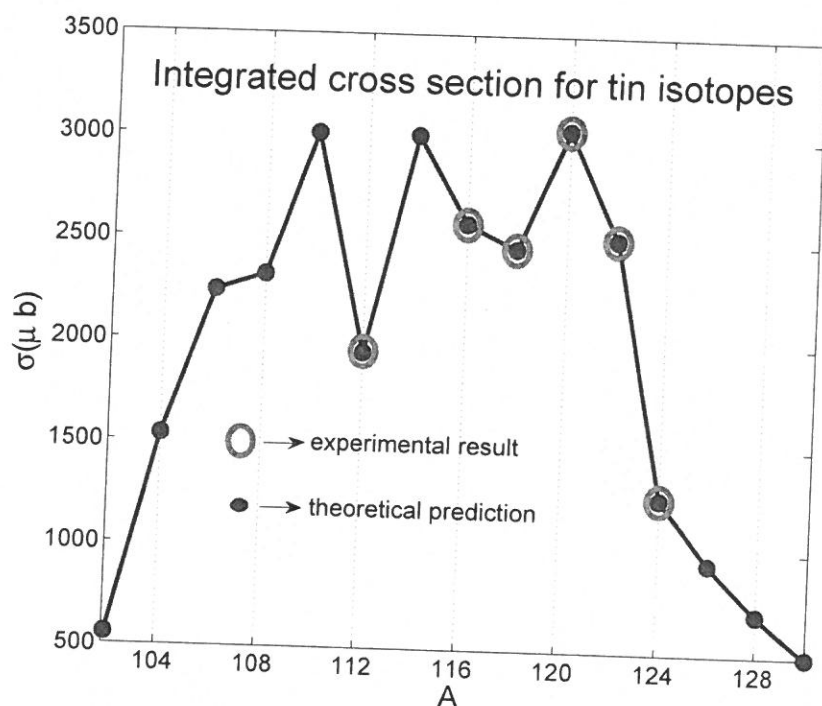
→ 13

Barranco et al. PR C 72/054314 (2005)
von Smas & Schuck

all
(I) and

1a
states

check
done



2.1.6
 Figure 2.2.1: Absolute value of the two-nucleon transfer cross section $^{A+2}\text{Sn}(p,t)^4\text{Sn}(\text{gs})$ ($A = 112, 116, 118, 120, 122, 124$ cf. Potel, G. et al. (2013a) Potel, G. et al. (2013b)) calculated taking into account successive and simultaneous transfer in second order DWBA, properly corrected for non-orthogonality contributions in comparison with the experimental data (Guazzoni, P. et al. (1999), Guazzoni, P. et al. (2004), Guazzoni, P. et al. (2006), Guazzoni, P. et al. (2008), Guazzoni, P. et al. (2011), Guazzoni, P. et al. (2012)).

renormalized by the degree of single-particle content of the levels where nucleons correlate. The quantity

$$N'(0) = Z_\omega^{-1} N(0) = (1 + \lambda) N(0) \quad (2.2.3)$$

is the similarly renormalized density of levels at the Fermi energy. From the above relations one obtains

$$x' = Z_\omega(v_p^{bare} + v_p^{ind})N(0). \quad (2.2.4)$$

All of the above many-body, ω -dependent effects which imply in many cases a coherent sum of amplitudes, are not simple to capture in a spectroscopic factor in connection with one-particle transfer, let alone two-nucleon transfer processes.¹⁴

In keeping with the fact that $m_k \approx 0.6 - 0.7m$ and that $m^* \approx m$, as testified by the satisfactory fitting standard Saxon-Woods potentials provides for the valence orbitals of nucleons of mass m around closed shells, one obtains $m_\omega \approx 1.4 - 1.7m$. Thus $Z_\omega \approx 0.6 - 0.7$. It is still an open question how much of the observed single-particle depopulation can be due to hard core effects, which shifts the associated strength to high momentum levels¹⁵ (cf. Dickhoff, W. and Van Neck (2005), Jennings, B. (2011), Kramer, G. J. et al. (2001), Barbieri, C. (2009), Schiffer, J. P. et al. (2012), Duguet, T. and Hagen (2012), Furnstahl, R. J. and Schwenk (2010)). An estimate of such an effect of about 20% will not quantitative change the long wavelength estimate of Z_ω given above. Arguably, a much larger depopulation through hard core effects remains an open problem within the overall picture of elementary modes of nuclear excitation and of medium polarization effects.

Mottelson (1998) Les Houches

2.3 Quantality Parameter

The quantality parameter (Nosanow (1976), de Boer (1957), de Boer (1948), de Boer and Lundbeck (1948))¹⁶ is defined as the ratio of the quantal kinetic energy of localization and potential energy, (cf. Fig. 2.3.1 and Table 2.3.1). Fluctuations, quantal or classical, favor symmetry: gases and liquids are homogeneous. Potential energy on the other hand prefers special arrangements: atoms like to be at specific distances and orientations from each other (spontaneous breaking of translational and of rotational symmetry reflecting the homogeneity and isotropy of empty space).¹⁷ Within this context cf. App 2.6, end of Sect. 2.6.1 as well as Sect. 6.2.3.¹⁸

When q is small, quantal effects are small and the lower state for $T < T_c$ will have a crystalline structure, T_c denoting the critical temperature. For sufficiently

¹⁶ Within this general context the physics embodied in the quantality parameter is closely related to that which is at the basis of the classical Lindemann criterion (Lindemann (1910)) to measure whether a system is ordered (e.g. a crystal) or disordered (e.g. a melted system) (Bilgram (1987), Löwen, H. (1994), Stillinger (1995)). The above statement is also true for the generalized Lindemann parameter (Stillinger and Stillinger (1990), Zhou et al. (1999)), used to provide similar insight into inhomogeneous finite systems like e.g. proteins (aperiodic crystals Schrödinger, E. (1944), see also Ehrenfest's theorem (Basdevant and Dalibard (2005) pag. 138)). See also App. 2.C

14

see Barranco et al (2005) viñas PRC 72, 054314

(2005)

15

16

constituents	M/M_n	$a(\text{cm})$	$v_0(\text{eV})$	q	phase($T = 0$)
${}^3\text{He}$	3	2.9(-8)	8.6(-4)	0.19	liquid ^{a)}
${}^4\text{He}$	4	2.9(-8)	8.6(-4)	0.14	liquid ^{a)}
H_2	2	3.3(-8)	32(-4)	0.06	solid ^{b)}
${}^{20}\text{Ne}$	20	3.1(-8)	31(-4)	0.007	solid ^{b)}
nucleons	1	9(-14)	100(+6)	0.5	liquid ^{a),c),d)}

0,4

Table 2.3.1: Zero temperature phase for a number of systems. a) delocalized (condensed), b) localized, c) non-Newtonian solid (cf. e.g. Bertsch (1988), de Gennes (1994), p. 25), that is, systems which react elastically to sudden solicitations and plastically under prolonged strain, d) paradigm of quantal, strongly fluctuating, finite many-body systems. While delocalization or less does not seem to depend much on whether one is dealing with fermions or bosons (Mottelson (1998) and refs. therein; cf also Ebran et al. (2014a), Ebran et al. (2014b), Ebran et al. (2013), Ebran et al. (2012)), the detailed properties of the corresponding single-particle motion are strongly dependent on the statistics obeyed by the associated particle (cf. App. 2.5).

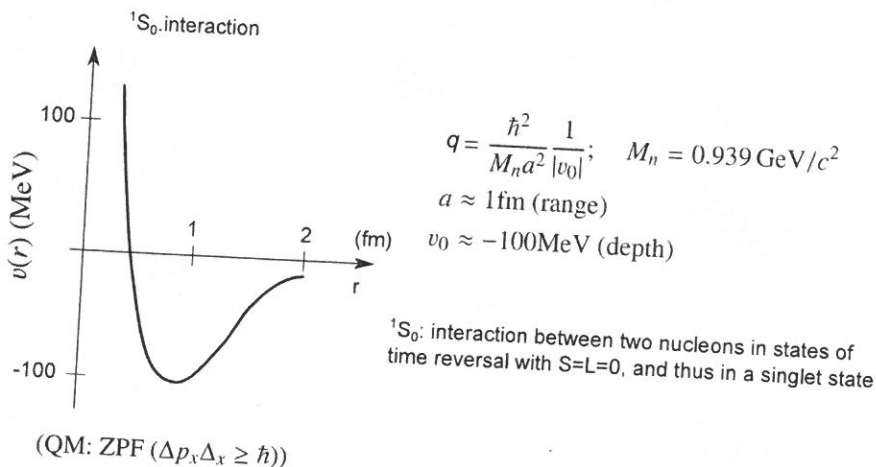


Figure 2.3.1: Schematic representation of the bare NN -interaction acting among nucleons displayed as a function of the relative coordinate $r = |\mathbf{r}_1 - \mathbf{r}_2|$, used to estimate the quantity parameter q , ratio of the zero point fluctuations (ZPF) of confinement and the potential energy.

2.3. QUANTITY PARAMETER

Namely confinement with long mean free path as compared with nuclear dimensions.¹⁷

large values of q (> 0.15) the system will display particle delocalization and, likely, be amenable, within some approximation, to a mean field description (Fig. 2.3.2 and Fig. 2.3.3) cf. also 2.6.3 and also Figs. 2.3.4 and 2.3.5). In fact, the step delocalization → mean field is certainly not automatic, neither guaranteed. In any case, not for all properties neither for all levels of the system. Let us elaborate on these points. It is arguably true that independent particle motion can be viewed as the most collective of all nuclear properties, reflecting the effect of all nucleons on a given one resulting in a macroscopic effect (confinement). Consequently, it should be possible to calculate the mean field in an accurate manner as the sum of many contributions whose relative errors cancel out, in average, against each other, an ansatz found at the basis of most collective approximations, like e.g. RPA. On the other hand, this fact does not guarantee that each single contribution is correctly calculated but, alas, the opposite. Thus, it will not be surprising that if one could force each, or at least a number of the virtual individual contributions to become real by acting with an appropriate external field (specific experiment), one would find varied degrees of agreement with experiment. Within this context one may find through mean field approximation a good description for the energy of the valence orbitals of a nucleus but for a specific level (e.g. the $d_{5/2}$ level of $^{119-120}\text{Sn}$, cf. e.g. Fig 4.2.3). It is not said that including particle-vibration coupling corrections, a process which in average makes theory come closer to experiment (cf. e.g. Bohr, A. and Mottelson (1975), Bortignon, P. F. et al. (1977), Mahaux, C. et al. (1985), Bès and Broglia (1971a), Bès and Broglia (1971b), Bès and Broglia (1971c), Bortignon et al. (1976), Bès, D. R. et al. (1988), Barranco et al. (1987), Barranco, F. et al. (2001) and references therein), single specific quasiparticle will agree better with the data (cf. also Tarpanov, D. et al. (2014)). Cases like this one constitute a sobering experience concerning the intricacies of the many-body problem in general, and the nuclear one (finite many-body system, FMBS) in particular. In other words, one is dealing with a self-confined, strongly interacting, finite many-body system generated from collisions originally associated with a variety of astrophysical events and thus with the coupling and interweaving of different scattering channels and resonances, a little bit as e.g. the Hoyle monopole resonance ($\alpha + \alpha + \alpha \rightarrow ^{12}\text{C}$). Within the anthropomorphic (grand design) scenario such phenomena are found in the evolution of the Universe to eventually allow for the presence of organic matter and, arguably, life on earth (cf. e.g. Rees, M. (2000), Meissner, U. G. (2014) and references therein) more likely than to make mean field approximation an "exact" description of nuclear structure and reactions.

Arguably, as accurately as one can calculate collective vibrations, e.g. quadrupole vibrations. But this does not mean that one knows how to correctly calculate the energy and associated deformation parameter of each single state of the quadrupole response function

17

18

19

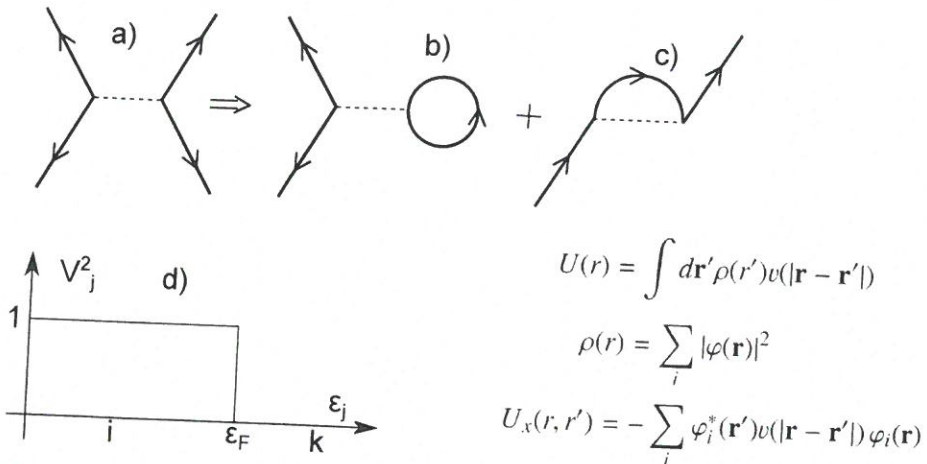


Figure 2.3.2: Schematic representation of (a) nucleon–nucleon scattering through the bare NN -interaction, (b) the associated contribution to the Hartree potential $U(r)$ and, (c) to the Fock (exchange) potential $U_x(r, r')$, $\rho(r)$ being the nucleon density. (d) the Hartree–Fock solution leads to a sharp discontinuity at the Fermi energy ϵ_F . That is, single-particle levels with energy $\epsilon_i \leq \epsilon_F$ are fully occupied. Those with $\epsilon_k \geq \epsilon_F$ empty.

2.4 Relation between collectivity and correlations

2.5 Quantality, Pauli principle, closed shells and single-particle motion

2.6 Cooper pairs

Let us assume that the motion of nucleons is described by the Hamiltonian,

$$H = \sum_{j_1 j_2} \langle j_1 | T | j_2 \rangle a_{j_1}^\dagger a_{j_2} + \frac{1}{4} \sum_{\substack{j_1 j_2 \\ j_3 j_4}} \langle j_1 j_2 | v | j_3 j_4 \rangle a_{j_2}^\dagger a_{j_1}^\dagger a_{j_3} a_{j_4}, \quad (2, 2, 1)$$

written in second quantization (cf. e.g. Brink, D. and Broglia (2005), App. A). In what follows it will be schematically shown how mean field is extracted from such a Hamiltonian, both in the case of single-particle motion (HF) and of independent pair motion (BCS).

2.6.1 independent-particle motion the previous section

In App. 2.3 it was shown that the value of the quantality parameter associated with nuclei ($q \approx 0.5$) leads to particle delocalization and likely makes the system amenable to a mean field description (Fig. 2.3.2; see however the provisos expressed at the end of App. 2.3). In such a case, Hartree–Fock approximation is

0, 4
slect.

*

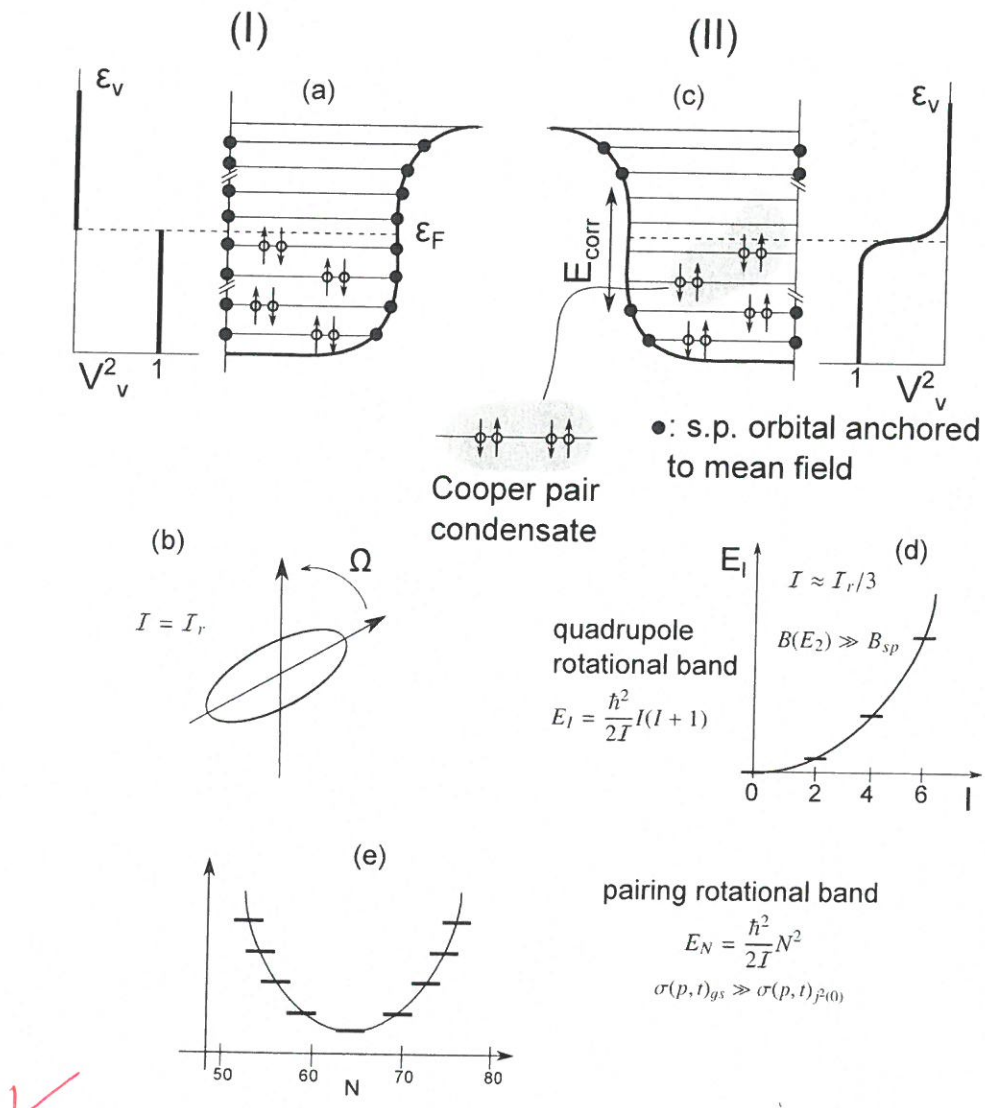


Figure 2.3.3: (I) (a) Schematic representation of “normal” (independent-particle) motion of nucleons in two-fold degenerate (Kramers, time-reversal degeneracy) orbits solidly anchored to the mean field and displaying a sharp, step-function-like, discontinuity in the occupancy at the Fermi energy lead to a deformed (Nilsson (1955)) rotating nucleus with a rigid moment of inertia I_r (b). (II) Schematic representation of independent nucleon Cooper pair motion in which few (of the order of 5-8) pairs lead to (c) a sigmoidal occupation transition at the Fermi energy and, having uncoupled themselves from the fermionic mean field being now (quasi) bosons they essentially do not contribute to (d) the moment of inertia of quadrupole rotational bands leading to $I \approx I_r/3$ (cf. Belyaev, S. T. (2013), Belyaev (1959), Bohr, A. and Mottelson (1975) and references therein), (e) pairing rotational bands in gauge space, an example of which is provided by the ground states of the superfluid Sn-isotopes (see also Figs. 2.1.3 and 2.1.4).

tantamount to a selfconsistent relation between density and potential, weighted by the nucleon-nucleon interaction v , and leading to a complete separation between occupied ($|i\rangle$) and empty ($|k\rangle$) states,

$$(U_\nu^2 + V_\nu^2) = 1; \quad |\varphi_\nu\rangle = \tilde{a}_\nu^\dagger |0\rangle = (U_\nu + V_\nu a_\nu^\dagger) |0\rangle; \quad V_\nu^2 = \begin{cases} 1 & \epsilon_i \leq \epsilon_F, \\ 0 & \epsilon_k > \epsilon_F. \end{cases} \quad (2.2.2)$$

The Hartree-Fock ground state can then be written as,

$$|HF\rangle = |\det(\varphi_\nu)\rangle = \Pi_\nu \tilde{a}_\nu^\dagger |0\rangle = \Pi_i a_i^\dagger |0\rangle = \Pi_{i>0} a_i^\dagger a_i^\dagger |0\rangle. \quad (2.2.3)$$

where $|\tilde{i}\rangle$ is the time reversed state to $|i\rangle$.

To be solved, the above self-consistent equations have to be given boundary conditions. In particular, make it explicit whether the system has a spherical or, for example, a quadrupole shape. That is, whether $\langle HF | Q_2 | HF \rangle$ is zero or has a finite value, $Q_{2M} = \sum_{j_1 j_2} \langle j_2 | r^2 Y_M^2 | j_1 \rangle [a_{j_1}^\dagger a_{j_2}]_M^2$ being the quadrupole operator which carries particle transfer quantum number $\beta = 0$, in keeping with its particle-hole character. In the case in which $\langle Q_{2M} \rangle = 0$, the system can display a spectrum of low-lying, large amplitude, collective quadrupole vibrations of frequency $(C/D)^{1/2}$, the associated ZPF = $(\hbar^2/(2D\hbar\omega))^{1/2}$ leading to dynamical violations of rotational invariance (cf. App. 2.4). In the case in which $\langle Q_{2M} \rangle \neq 0$, the $|HF\rangle$ state is known as the Nilsson state, $|\text{Nilsson}\rangle$, defining a privileged orientation in 3D-space and thus an intrinsic, body-fixed system of reference K' which makes an angle Ω (Euler angles) with the laboratory frame K (Nilsson (1955)). Because there is no restoring force associated with the different orientations, fluctuations in Ω diverge in just the right way to lead to a rotational band displaying a rigid moment of inertia (cf. Fig. 2.3.3), and whose members are the states (Bohr, A. and Mottelson (1975)), and 2.6.1

$$|IKM\rangle \sim \int d\Omega \mathcal{D}_{MK}'(\Omega) |\text{Nilsson}(\Omega)\rangle; \quad E_I = (\hbar^2/2I) I(I+1); \quad I = I_{\text{rig}}. \quad (2.2.4)$$

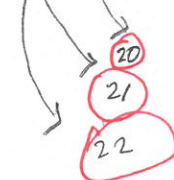
One can also view such bands as the limit ($C \rightarrow 0, D (= I)$ finite) of low energy ($\omega \rightarrow 0$), large-amplitude collective vibration (see App. 2.4). Similar dynamic and static spontaneous symmetry breaking phenomena take place in connection with particle-particle ($\beta = +2$ transfer quantum number) and hole-hole ($\beta = -2$) correlations, namely in gauge space (see Fig. 2.6.1; subject discussed also in App. 2.7 (dynamic: pairing vibration) and also below (static: pairing rotation); see also Figs. 2.1.1, 2.1.3 and 2.1.4). For a consistent discussion of these subjects, see Bès, D. R. and Kurchan (1990).

Sect.

2.6.2 independent-pair motion

Let us make use of the constant pairing matrix element approximation $\langle j_1 j_2 | v | j_3 j_4 \rangle = G$, that is,

$$H_P = -G \sum_{\nu, \nu' > 0} a_\nu^\dagger a_{\nu'}^\dagger a_\nu a_{\nu'}. \quad (2.2.5)$$



The abnormal density mean field (cf. e.g. Figs. 2.6.2 and 2.6.3) is related to the finite value of the pair operator, that is,

$$\sum \langle a_{j_2}^\dagger a_{j_1}^\dagger \rangle a_{j_3} a_{j_4} + \sum a_{j_2}^\dagger a_{j_1}^\dagger \langle a_{j_3} a_{j_4} \rangle; |\varphi_{jm}^{\text{COOPER}}\rangle = (U_j + V_j a_{jm}^\dagger a_{\tilde{j}m}^\dagger) |0\rangle,$$

the ground (mean field) state being,

$$|BCS\rangle = \prod_{jm>0} (U_j + V_j a_{jm}^\dagger a_{\tilde{j}m}^\dagger) |0\rangle; \alpha_0 = \langle BCS | \sum_{jm>0} a_{jm}^\dagger a_{\tilde{j}m}^\dagger | BCS \rangle.$$

(2)-124

Let us introduce the phasing (cf. e.g. Schrieffer, J. R. (1973)),

$$U_\nu = |U_\nu| = U'_\nu; \quad V_\nu = e^{-2i\phi} V'_\nu; \quad (V'_\nu \equiv |V_\nu|) (\nu \equiv j, m),$$

F. 2.2.8)

where ϕ is the gauge angle. One can then write the (BCS) wavefunction as,

$$|BCS(\phi)\rangle_K = \prod_{\nu>0} (U'_\nu + V'_\nu e^{-2i\phi} a_\nu^\dagger a_{\bar{\nu}}^\dagger) |0\rangle = \prod_{\nu>0} (U'_\nu + V'_\nu a_\nu^{\dagger'} a_{\bar{\nu}}^{\dagger'}) |0\rangle \quad (2.2.9)$$

$$= |BCS(\phi = 0)\rangle_{K'} : \text{lab. system, } K : \text{intr. system } K',$$

where $a_\nu^{\dagger'} = e^{-i\phi} a_\nu^\dagger$ is the single-particle creation operator referred to the intrinsic system. The BCS number and gap equations, order parameter, and two-nucleon spectroscopic amplitudes are,

$$\langle BCS | \sum_{\nu>0} a_\nu^\dagger a_{\bar{\nu}}^\dagger | BCS \rangle$$

$$= \alpha_0 = \alpha'_0 e^{-2i\phi}; \quad \alpha'_0 = \sum_{\nu>0} U'_\nu V'_\nu; \quad \Delta = G\alpha_0, \quad (2.2.10)$$

$$B_\nu = \langle BCS | \frac{[a_\nu^\dagger a_{\bar{\nu}}^\dagger]_0}{\sqrt{2}} | BCS \rangle = (j_\nu + 1/2)^{1/2} U'_\nu V'_\nu,$$

and

$$N_0 = 2 \sum_{\nu>0} V_\nu^2; \quad \frac{1}{G} = \sum_{\nu>0} \frac{1}{2E_\nu} \cdot \left(\frac{V'_\nu}{U'_\nu} \right) = \frac{1}{\sqrt{2}} \left(1 \mp \frac{1}{E_\nu} \right)^{1/2}. \quad (2.2.11)$$

Examples of B_ν -coefficients for the reaction $^{124}\text{Sn}(p, t)^{122}\text{Sn}$ (gs) are given in Table 2.6.1.

The wavefunction and energies of the members of the pairing rotational band, can be written as

$$|N_0\rangle \sim \int_0^{2\pi} d\phi e^{-iN_0\phi} |BCS(\phi)\rangle_K \sim \left(\sum_{\nu>0} c_\nu a_\nu^\dagger a_{\bar{\nu}}^\dagger \right)^{N_0/2} |0\rangle; \quad (2.2.12)$$

$$E_N = (\hbar^2/2I)N^2; \quad I \approx 2\hbar^2/G,$$

respectively (cf. e.g. Brink, D. and Broglia (2005) App. H).

23

(P) The abnormal density is related to the finite value of the pair operator. The associate independent pair states are written in the BCS approximation as

$$(U_\nu^2 + V_\nu^2) = 1 ; |Q_{\nu\bar{\nu}}\rangle = (U_\nu + V_\nu a_\nu^\dagger a_{\bar{\nu}}^\dagger) |10\rangle, \frac{V_\nu}{U_\nu} \Big] = \frac{1}{\sqrt{2}} \left(1 + \frac{E_\nu}{E_F} \right)^{1/2}$$

where $E_\nu = \sqrt{E_F^2 + \Delta^2}$ and $\epsilon_\nu = \epsilon_F - \lambda$, $\lambda = E_F$. (2.2.6)

The BCS ground state

$$|BCS\rangle = \prod_{\nu>0} (U_\nu + V_\nu a_\nu^\dagger a_{\bar{\nu}}^\dagger) |10\rangle \quad (2.2.7)$$

describes independent pair motion.

p. 124

(P)